JOURNAL OF MATERIALS SCIENCE 26 (1991) 3343–3353

Self-propagating high-temperature synthesis of molybdenum disilicide

S. C. DEEVI*
Department of Mechanical Engineering, University of California, Davis, CA 95616, USA

Molybdenum disilicide was synthesized from elemental reactants in argon and vacuum atmospheres by utilizing the exothermicity of the reaction using self-propagating high temperature synthesis. Experiments were carried out using powdered reactants and compacts with varying densities. The reaction front propagated at a finite velocity depending upon the atmosphere, the diameter of the pellet and the particle sizes of the reactants. The exothermicity of the reaction between molybdenum and silicon raised the temperature of the product to 1886 K, which is close to the theoretical adiabatic combustion temperature, 1900 K. X-ray diffraction analysis of the product confirmed the product to be a single phase $MoSi_2$ crystallizing in a tetragonal structure. Microstructural examination revealed melting of Si and its capillary flow, and chemical analysis indicated that the product is much purer than the reactants.

1. Introduction

Self-propagating reactions between solids are diverse in chemical nature, with the common property that the process is highly exothermic. A strong exothermic reaction at the surface liberates enough heat to heat the adjacent layer of reactants and the reaction becomes self-sustained. Spice and Staveley [1, 2] were the first to describe self-propagating solid-state reactions. Later, Booth [3] proposed a mathematical model describing the process. During the 1970s Merzhanov *et al.* and others [4–6] noticed an exceptionally interesting process of heterogeneous combustion between metals, metal–non-metal, and metal-reacting gas without the presence of oxygen. Their investigations led to manufacturing processes to synthesize refractory materials such as alloys, transition metal borides, carbides, silicides and nitrides. The process has since been referred to as combustion synthesis or self-propagating high temperature synthesis (SHS). The SHS technique has generated great interest [7–9] due to the short reaction times and high purity of the products.

The reaction between molybdenum and silicon to form molybdenum disilicide is exothermic with a ΔH value of 31.4 kcal per Mo atom. Of the silicides, molybdenum disilicide ($MoSi_2$) has gained industrial importance [10–13] due to its high melting point, high emissivity, stable resistance over long periods of time, and the ability to form a self-healing protective layer. A cermet of $MoSi_2$ (90% $MoSi_2$ + 10% metal) is an important industrial heating element for use in oxygen as compared to heating elements made from superalloys, metals and graphite. There is a growing interest to use $MoSi_2$ as an "instant heater" cooker-top unit in place of traditional tubular heating elements [14]. Industrially, $MoSi_2$ was first produced [15] using a thermite mix. At a later stage an approach involving melting, sintering and hot pressing was taken towards the synthesis of $MoSi_2$ in a hydrogen atmosphere [16, 17]. Most of the above processes require high temperature industrial furnaces, and the product obtained must be properly heat treated to ensure a homogeneous product. The risk of contamination is also a common concern with the industrial process. Although some of the earlier workers reported the synthesis of $MoSi_2$ from the elements [12, 18–20], Sarkisyan *et al.* [21] reported combustion synthesis of several transition metal silicides and present the only discussion, albeit brief, of the synthesis of the molybdenum silicides.

The present work was undertaken to study in greater detail the various parameters affecting the synthesis of $MoSi_2$. Although heat of reaction or exothermicity of a system is an important factor in the conversion of reactants to products, other parameters such as particle size, sample size and sample atmosphere play a significant role in the synthesis of molybdenum silicides. The present investigation aims at establishing physical parameters controlling the conversion of reactants to products, and at understanding the mechanism/s involved in the synthesis of molybdenum disilicide. The study is extended to issues such as compositional consistency, microstructure, product homogeneity, and surface structure.

2. Experimental procedure

Molybdenum (Mo) and silicon (Si) powders used in the present work were as-received powders obtained from Alfa products (Ward Hill, MA) and Aldrich chemical company (Milwaukea, WI). The Mo powders were 4 to 8, < 63, and < 150 μm, and Si powders

* *Present address*: Research & Development Center, Philip Morris, USA, P.O. Box 26583, Richmond, Virginia 23261, USA.

0022–2461/91 $03.00 + .12

were < 47, < 150, and < 300 μm (Table I). The powders were thoroughly mixed in the desired ratio (atomic ratio of Si/Mo = 2) in an ultrasonic mixer and also by hand-mixing in a slurry made with an organic solvent. Since mixing is an essential step in obtaining a product with a homogeneous composition, much care was taken to avoid segregation of one particular component which may lead to micro- or macro-segregation in the final product. The slurry was dried in air followed by vacuum drying. Pellets were made in a die-steel die with two plungers by using a hydraulic press to press the powder mixtures. Pelletizing pressure and the weight of the samples were varied in the range 70 to 600 MPa and 10 to 20 g, respectively, depending upon the diameter of the pellet. Pressures were applied uniaxially on the powder mixture on both sides of the compact and the pressure was kept constant on each side for 3 min. This precaution enabled us to obtain cylindrical compacts of approximately 30 mm in length without any apparent density differences across the length and diameter of the compact.

A schematic of the experimental apparatus used for synthesizing molybdenum silicides is shown in Fig. 1.

TABLE I Characteristics of powders employed

Powder	Powder sizes (μm)	Average particle size (μm)	Surface area ($m^2 g^{-1}$)
Mo[a]	4–8	5.7	0.33
	< 63	13.3	0.20
	< 150	18.6	0.18
Si	< 47	12.6	2.15
	< 150	43.5	0.37
	< 300	79.1	0.12

[a]Aldrich chemical company.

Experiments were carried out in a stainless steel chamber with two 12.5 cm quartz windows. A cylindrical pellet was placed on a boron nitride or quartz disk with an ignition coil located on the upper surface of the compact. The chamber was sealed and evacuated to 5 μm vacuum. After flushing with argon, the chamber was evacuated again, and at this point experiments were carried out either in a stagnant vacuum of 5 to 10 μm or stagnant argon pressure of 1.2 atm. Ignition was achieved by supplying a pulse of current to the ignition coil for a few seconds.

Combustion wave velocities were obtained by noting the time involved for the reaction front to propagate along a certain length of the compact. Ignition and temperature profiles were recorded using tungsten–5% rhenium against tungsten–26% rhenium thermocouples by placing thermocouples as shown in Fig. 2. The thermocouple arrangement indicated in Fig. 2a was used for ignition temperature profiles. A small groove was cut on the surface of the compact and the thermocouple bead was placed in it. A very fine layer of the powder with the same composition as that of the compact was spread onto the thermocouple covering the bead of the thermocouple. Fig. 2b indicates the thermocouple arrangement used for measuring the temperature profile of the compact during the combustion wave propagation. The thermocouple was forced against the compact and the thermocouple hole was filled with the same powder as that of the compact to minimize heat losses and any errors that may be introduced in the measured reaction temperature. In certain cases, thermocouples were located away from the ignition source and from the bottom sample supporting the arrangement. Combustion wave velocities were obtained by noting the time involved for the reaction front to propagate from the top thermocouple to the bottom thermocouple. Ignition and temperature profiles were recorded

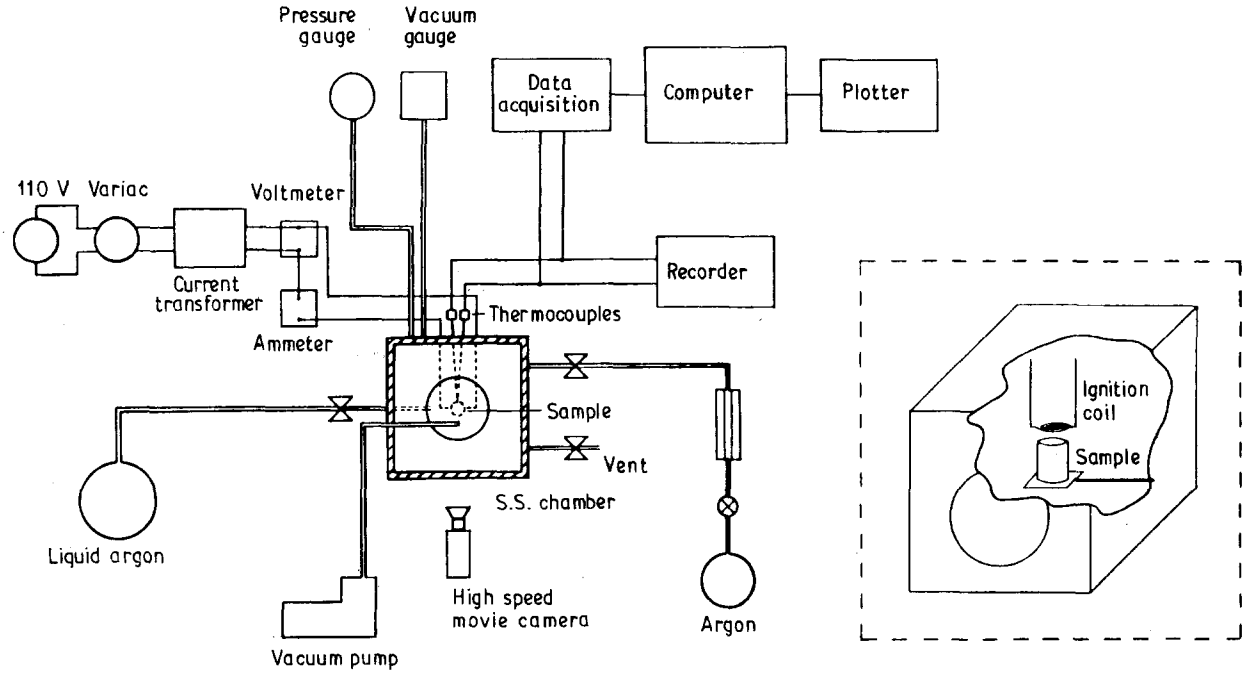

Figure 1 Schematic of experimental apparatus used for combustion synthesis of $MoSi_2$.

Figure 2 Thermocouple arrangements used for obtaining ignition and temperature profiles (a–c) see text.

using 167 μm bead tungsten–5% rhenium against tungsten–26% rhenium thermocouples. This technique enabled us to determine the temperatures within 100 ms. A spectroradiometer was also used to determine the wavelength of the emitted radiation from which the combustion temperature was calculated.

X-ray diffractograms were obtained on a Norelco diffractometer unit with a vertical goniometer arrangement using CuK_α radiation at 35 kV and 15 mA with a nickel filter. In the case of combustion-synthesized samples, a cylindrical sample was sliced along its radial direction and the unground sample was subjected to the analysis. Powders were also obtained from several portions of the sample to identify the product phases and the original reactants.

3. Results

Cylindrical compacts of Mo–Si mixture in the composition corresponding to $MoSi_2$ ignited easily after a sufficient amount of radiant energy from the ignition coil was received by the surface layer of the compact. Ignition occurred on the compact as a spot and quickly spread to the entire cross-sectional area of the compact. The combustion wave propagated along the length of the compact as indicated in Fig. 3. The luminous bright zone in Fig. 3a is due to the ignition coil prior to the ignition. The bright moving zone on the upper portion of the compact separated the reactants from the products and moved at a finite velocity depending upon the atmosphere, particle sizes of the powders and densities of the compact, as will be discussed below. The reaction front propagated through the reactants as indicated sequentially in Fig. 3 until all the reactants were consumed. The sample was bright for a much longer time even after the reaction front propagated through the reactants. The length and volume of the sample increased at the end of the reaction and the product had a layered appearance, as will be described later.

Fig. 4 indicates the variation of combustion velocity, defined as the rate at which the reaction front moves, with percentage theoretical maximum density (TMD) of 19.6 mm diameter compact in an argon atmosphere and in vacuum. Note that the compacts are quite porous and the percentage TMD ranges from 30 to 55%. According to Fig. 4, combustion velocity varies linearly and the combustion velocities of compacts are higher in argon as compared to vacuum. Argon samples were reacted at 1.2 atm (912 mm of Hg) of argon pressure as opposed to 5×10^{-3} to 10×10^{-3} mm Hg pressure in vacuum. A decrease in the diameter of the compact to 12.5 mm also reduces the combustion velocity as may be noted from Fig. 5. Decreasing the diameter from 19.6 to 12.5 mm increases the surface area to volume ratio by 36%, resulting in an increase in the heat losses.

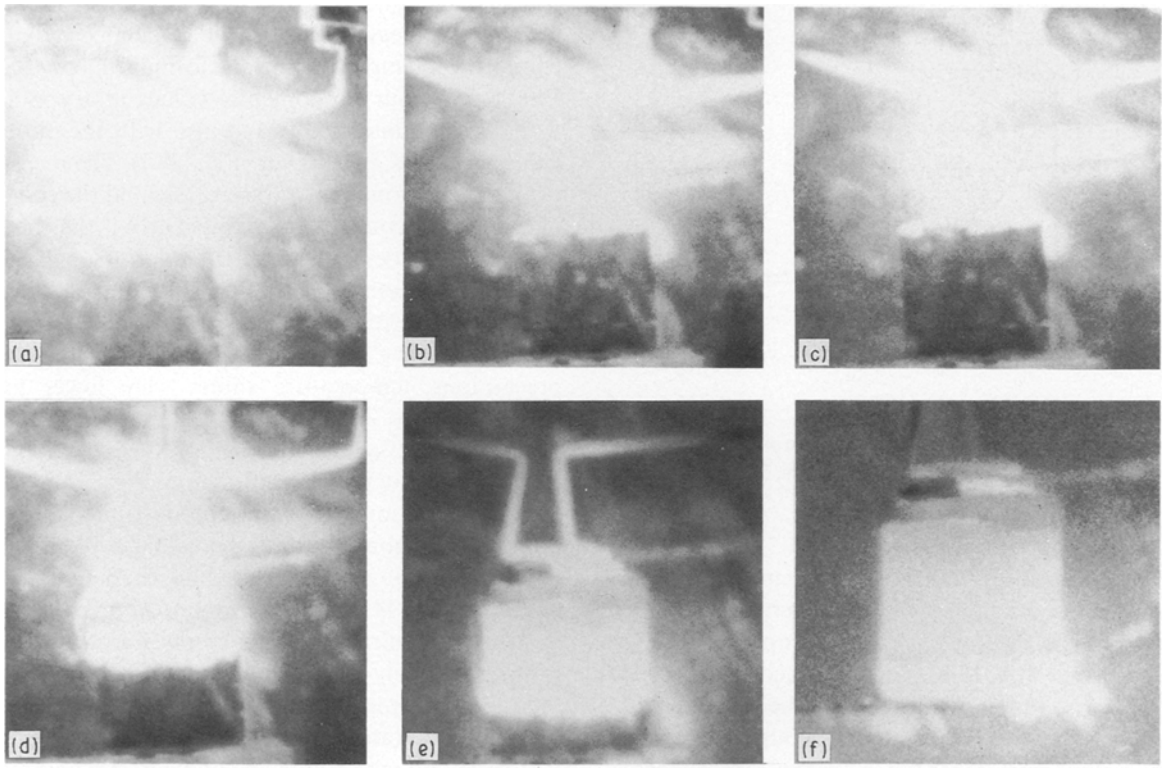

Figure 3 Propagation of the combustion wave through the reactants corresponding to the composition of $MoSi_2$. (a) Prior to ignition, luminous bright zone is due to the ignition coil. (b–e) Sequential photographs obtained during the propagation of the combustion wave. Note the movement of a glowing zone in (b–e). The glowing front separates the product from the reactants ahead of the front. (f) Photographs obtained during the cool-down period.

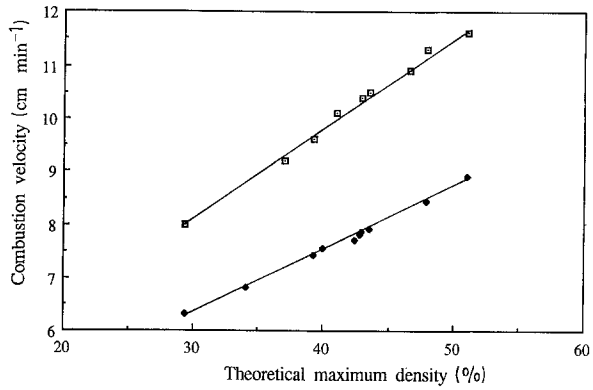

Figure 4 Experimentally observed dependence of combustion velocities with percentage TMD of the compacts in ⊡ argon (1.2 atm) and ◆ vacuum (5 μm) atmospheres. Mo < 63 μm, Si < 44 μm, diameter 19.6 μm.

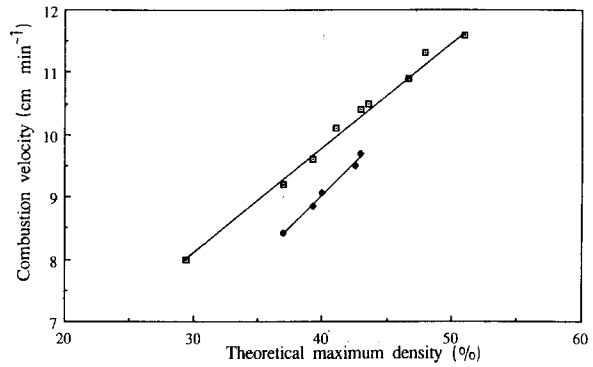

Figure 5 Effect of diameter of the compact and percentage TMD on the combustion velocities. Diameters ⊡ 19.6 μm, ◆ 12.5 μm. Mo < 63 μm, Si < 47 μm, argon atmosphere.

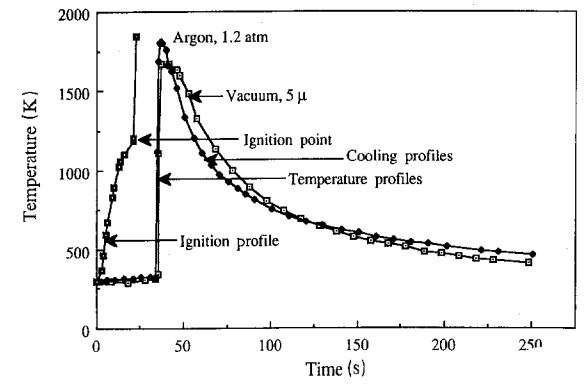

Figure 6 Traces of ignition and temperature profiles in argon and vacuum atmospheres. Mo < 63 μm, Si < 47 μm, %TMD 42.5.

A typical ignition (in argon) and temperature profiles obtained both in argon and vacuum are indicated in Fig. 6. Note the sudden rise of temperature in the ignition profile at 1217 K. The thermocouple recorded an abrupt rise in temperature when the reaction front was at the location of the thermocouple. The maximum temperature recorded in argon atmosphere is 1886 K while the maximum temperature recorded in vacuum is 1690 K, lower by 196 K. In both cases, the sample cools immediately and the cooling takes a finite time. The sample glowed for a much longer time (50 s) as compared to the heating time involved during combustion. Heating rates calculated in argon and vacuum are 48 000 and 37 000 K min^{-1}, respectively. The heating rates involved in this technique are substantially higher than in any conventional process. Average cooling rates are in the range of 400–800 K min^{-1}.

The maximum combustion temperature recorded in vacuum is lower, and the temperature remained at that value for 7 s (Fig. 6). The specific heat of the product and the calculated combustion temperatures of the three products are indicated in Table II. Thermodynamically, the maximum attainable temperature is the calculated adiabatic combustion temperature as dictated by the heat of formation and specific heat of the product. Therefore, the observed temperature should be close to the adiabatic combustion temperature if heat losses are negligible, and if both Mo and Si particles participate giving rise to a homogeneous single product, $MoSi_2$.

The maximum combustion temperature of 19.6 mm diameter compact was checked using a spectroradiometer. Measurement was carried out by focusing the spectroradiometer into a small hole drilled at the midpoint of the compact. The use of the spectroradiometer permitted measurement of spectral energy distribution throughout the visible and into the infrared region (from 390 to 1070 nm). During the propagation of the combustion wave, the temperature calculated from the spectral energy distribution corresponded to a temperature of 1900 K. During the cool-down period, the energy distribution shifted towards infrared, peaking in the infrared region. The maximum combustion temperature obtained with the thermocouple technique (Fig. 6) agrees with the spectroradiometer measurement. The calculated adiabatic combustion temperature in the formation of $MoSi_2$ is 1900 K, and our experimental values in argon agree with the calculated value and also with the observed value of 1900 K (Sarkisyan *et al.* [21]). The measured peak combustion temperature values and the response of the thermocouple vary significantly if the thermocouple bead does not touch the interior of the compact. A slight compressive force, and filling up the hole with the same reactants, increased the accuracy and response of the thermocouple. Without the above precautions, temperature values were lower by as much as 150 to 200 °C.

Combustion-synthesized samples were characterized using X-ray powder diffraction. Fig. 7 depicts the typical diffraction pattern of combustion-synthesized samples in argon when the percentage TMD of the compact is above 43% (Mo and Si powders were < 63 and < 44 μm, respectively). As can be noted from the diffractogram, combustion-synthesized $MoSi_2$ is highly crystalline and pure, without any reflections corresponding to either of the reactants. The diffractogram was obtained by exposing the surface of a 19.6 mm diameter compact. An analysis of several combustion-synthesized samples indicates that the diffraction patterns agree well with the standard pattern for $MoSi_2$ [22]. The unit cell parameters calculated from Fig. 7 are $a_0 = 0.320$ nm and

TABLE II Thermodynamic properties of molybdenum silicides

Property	$MoSi_2$	Mo_5Si_3	Mo_3Si
ΔH°_{298} (Kcal Mo atom^{-1})	− 31.4	− 13.4	− 8.0
ΔS°_{298} (Cal Mol °C)	8.67	1.91	0.38
C_p (solid) (Cal Mol °C)	$16.2 + 2.86 \times 10^{-3} T - 1.57 \times 10^5 T^{-2}$	$43.8 - 8.4 \times 10^{-3} T - 2.86 \times 10^5 T^{-2}$	$20.5 + 5.42 \times 10^{-3} T + 0.07 \times 10^5 T^{-2}$
Adiabatic temperature (K)	1900	1599	1200
Melting point (K)	2293	2453	2298

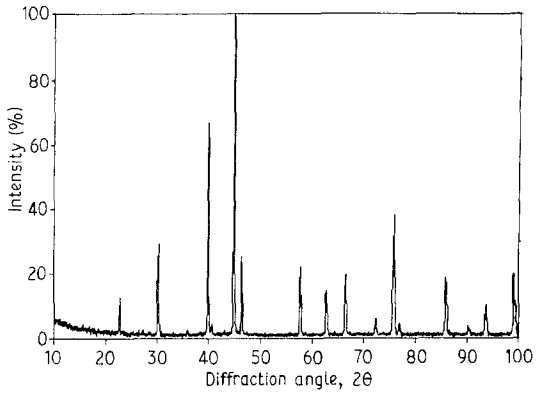

Figure 7 X-ray diffraction pattern of combustion-synthesized $MoSi_2$.

$c_0 = 0.784$ nm with unit cell volume corresponding to 8.033×10^{-23} cm^3. Since a unit cell of $MoSi_2$ consists of two molybdenum and four silicon atoms, as per Pauling [23], the calculated X-ray density corresponds to 6.29 g cm^{-3}. Unit cell volume and X-ray density calculated from the standard pattern of IJCPDS [22] correspond to 8.038×10^{-23} cm^3 and 6.28 g cm^{-3}, respectively. The pycnometric density value obtained with helium is 6.27 g cm^{-3} and agrees well with the X-ray density value and with the reported pycnometric density values [24].

Powdered mixture when reacted in a quartz crucible without compaction indicated several small portions of unreacted areas although the combustion wave propagated through the entire mixture. The reaction propagated irregularly unlike the propagation of the combustion wave as shown in Fig. 3. This behaviour with the reactant mixture has been observed in vacuum and in argon atmospheres. In some instances the wave propagated down at an angle, converting the reactants to product and then engulfing the unreacted portion with a combustion wave. This is attributable to the poor particle–particle contact associated with the voids.

The product obtained in quartz crucibles was a fused mass with strongly bonded particles (although powdered mixture was used instead of a compact) and assumed the shape of the crucible. The product exhibited rather poor conversion (both in argon and vacuum atmospheres) owing to the heat losses to the quartz crucible. The entire outer surface area and the bottom portion of the product had a layer of reactants with a thickness of about 1 mm. Due to the low density of the reactant material in the quartz crucibles, localized unreacted portions with an area of 2–6 mm^2 were observed in the interior of the product. Conversion was poor and only about 80–85% of the reactants were converted. Even though localized, unreacted material was observed in the interior of the product, the combustion wave propagated through the length of the quartz crucible.

To illustrate the effect of atmosphere and heat losses, combustion-synthesized samples in argon and vacuum were subjected to quantitative X-ray analysis. The compact densities were 42.5% TMD (diameter = 19.6 mm) and the Mo and Si powders were < 63 and < 44 μm, respectively. Powders scraped from the top most layer, the sides at mid-point of the compact and the bottom portion of the compact were analysed under the same conditions by integrating the peak areas. The top portions of the compacts in general showed reflections corresponding to only $MoSi_2$, and the conversion was 100%. The powders obtained from the sides of the compact indicated that 10.2% of the reactants were left in vacuum while only 1.5% of reactants were noticed in argon. Powders obtained from the bottom portions of the compact indicated the same trend as above except that the unreacted material increased to 14.3% (vacuum) and 3.3% (argon), respectively. Note that the combustion velocities and the observed combustion temperatures are lower in vacuum as compared to argon atmosphere.

When 20 g of reacted compacts were ground and analysed (% TMD of the compacts lay in the range 42 to 46% prior to combustion), conversion in argon and vacuum are 100 and 90%, respectively (note that the X-ray powder diffraction technique cannot distinguish minor phases below 2% when a single phase $MoSi_2$ is dominant). If Mo and Si reactants were to give 100% product, the observed temperature of the compact should be close to the adiabatic combustion temperature, 1900 K. Based on the 90% conversion efficiency, the estimated temperature rise should be around 1710 K and the observed temperature in vacuum is 1696 K. We have not observed such a close agreement

when the experiments were carried out with highly exothermic systems such as Ti–C or Ti–B, whose adiabatic temperatures are either close to 3000 K or higher.

The inability of the X-ray diffraction technique to reveal minor phases or unreacted elements below $\sim 2\%$ makes microstructural examination an essential component in the characterization of combustion-synthesized materials. It is necessary to estimate the amount of unreacted portions, if any, along with microsegregated areas since they will have a bearing on the electrical, thermal and mechanical properties of the synthesized product. To understand the microstructure, homogeneity and porosity of the synthesized $MoSi_2$ compacts, compacts were cut radially and longitudinally for examination under optical and scanning electron microscopes. Compacts with low densities often exhibited pores, unreacted areas surrounded by $MoSi_2$, and dense areas. Fig. 8a represents the features like open porosity at sites indicated by (a), unreacted components (b), segregated areas (c), and dense $MoSi_2$ product. Note that the diameter of the compact was 19.6 mm and the sample was polished. An interesting observation has been the segregated areas such as the ones indicated in Fig. 8 at sites indicated by (c), and the open porosity around the segregated areas. The porosity around the area may have been caused after the solidification of the segregated area around the matrix of $MoSi_2$ product. This can be clearly seen in the scanning electron micrograph (Fig. 8b) at a higher magnification. The surrounding matrix has been identified with EDAX as consisting of $MoSi_2$ particles and the dark area in the centre of the photograph as microsegregated silicon embedded with $MoSi_2$ particles on the surface. A clear separation of microsegregated area from the surrounding matrix can be seen in the micrograph. Visually, segregated areas have a steel greyish lustre, characteristic of silicon, while the surrounding $MoSi_2$ matrix has a grey colour.

Self-purification of the combustion synthesis technique may be understood from the reduction of impurities in the synthesized product as compared to the reactants (Table III). Low melting impurities like Na, K, S, Mg, Al and Ca either evaporated fully or showed a large reduction after the combustion synthesis had been carried out. This implies that most of the low melting impurities volatilize (either fully or partially) due to their high vapour pressures at the temperatures involved in the combustion synthesis process. A striking feature of Table III is the significant reduction of oxygen impurity in the synthesized powders either due to the desorption of chemisorbed oxygen on the reactants or due to partial volatilization of oxide impurities. A reducing atmosphere such as hydrogen may eliminate the residual oxygen content. The results indicate that the combustion synthesis technique leads to the development of ceramic materials with smaller amounts of impurities, which should improve their high temperature strength, spall, oxidation and corrosion resistance.

A longitudinally cut specimen (percentage TMD of the compact prior to the synthesis is 42%) as shown in

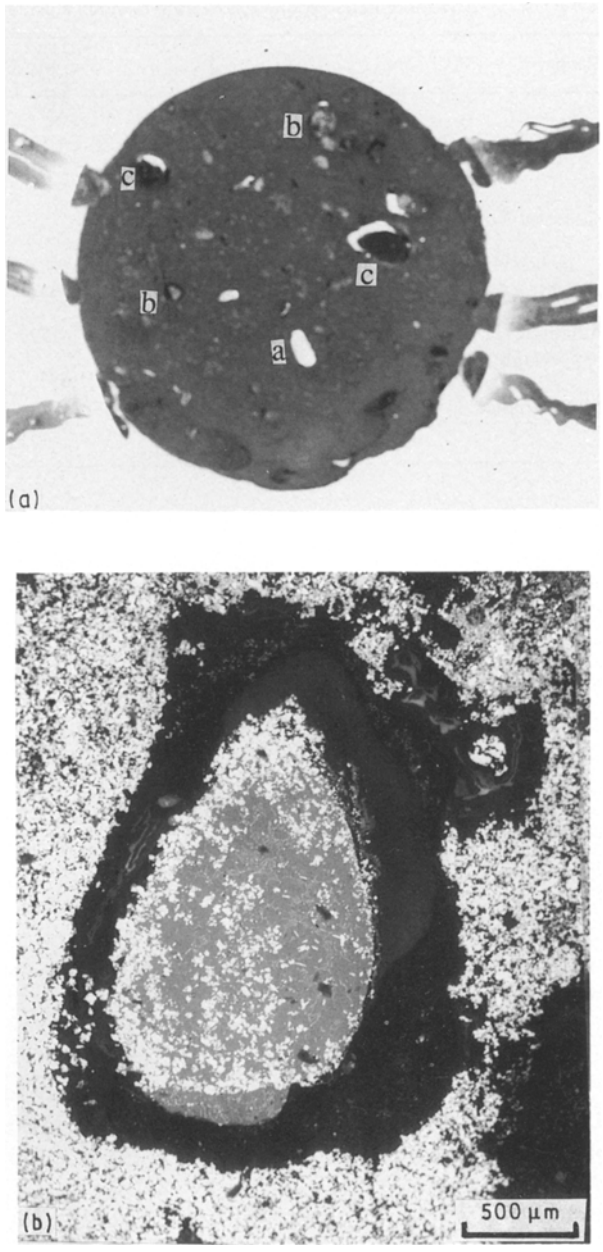

Figure 8(a) Optical micrograph of a radially sliced combustion-synthesized $MoSi_2$ compact. Sites (a) indicate open porosity, sites (b) indicate unreacted components, and sites (c) indicate microsegregated areas. (b) SEM of a microsegregated area. The inner portion of the micrograph is microsegregated Si embedded with $MoSi_2$ particles. Melting of Si followed by solidification resulted in this unique structure. The segregated area has a steel greyish lustre characteristic of Si.

Fig. 9 also indicated some cavities, cracks and some unreacted portions. The cracks may have been due to the expansion of the compact due to the expulsion of adsorbed gases. Surprisingly, unreacted portions and segregated areas were scattered without any apparent regularity either as to their location (radially and longitudinally) or as to the total size of unreacted portions. The unreacted portions were invariably surrounded by spherical voids, and can be seen due to the characteristic brownish colour of the reactants, as distinguished from the surrounding $MoSi_2$ product which is grey. A scanning electron micrograph of an island of unreacted Si and Mo particles surrounded by a matrix of $MoSi_2$ product is shown in Fig. 10a. One

TABLE III Chemical analysis of combustion-synthesized $MoSi_2$ in argon atmosphere

Element	Melting point (°C)	Composition (wt %)		
		Reactants		Product
		Mo	Si	$MoSi_2$
H	—	700	1900	500
N	—	—	—	100
O	—	4700	10 000	2200
Na	97.8	< 5	ND	ND
Mg	650	1	20	ND
S	119	1200	500	400
K	637	< 21	—	ND
Ca	838	6	200	100
Al	660	20	600	100
Fe	1536	88	2000	527
Cu	1083	8	20	16
Ni	1453	73	40	77
Cr	1875	28	100	ND
Ti	168	—	200	ND
W	3410	100	—	ND

ND = Not detectable.

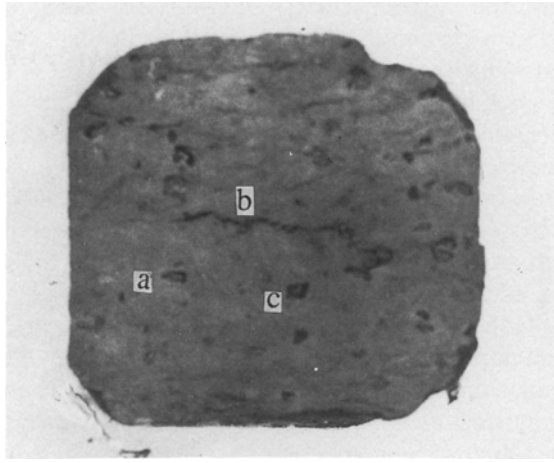

Figure 9 Optical micrograph of a longitudinally sliced combustion-synthesized $MoSi_2$ compact. Sites (a) indicate cross-sectional view of cavities, sites (b) indicate cracks generated due to the expansion of the compact during the expulsion of adsorbed gases and $MoSi_2$ product layer formation, and sites (c) indicate unreacted portions with brownish colour.

of the most striking features of the micrograph is the appearance of a melt layer or froth at the arrow mark. Spreading of the melt layer and wetting of the particles can be seen clearly in Fig. 10b. The length of the melt layer is at least 400 μm (Fig. 10a) without any discontinuity, while the particle size of Si certainly did not exceed 47 μm. Also note the channels among the pores at sites indicated by the pointers. This is a direct confirmation of melting of Si and its capillary flow along the pores of Mo particles. Particles of Mo retained their original shape which is reflected in Fig. 10b and Fig. 10c.

The macroporosity and the flaws in the synthesized compacts are negligible considering that the original compacts had more than 50% porosity. One of the main reasons is that the volume of Si particles in a compact is at least four times higher (the density of Si is 2.33 $g\,cm^{-3}$ while the density of Mo is 10.2 $g\,cm^{-3}$) even though the silicon content on a weight basis is only 36.9%. During the combustion synthesis reaction, melting of Si and its capillary flow along the channels of pores and around Mo particles forms a $MoSi_2$ layer whose specific volume is much higher

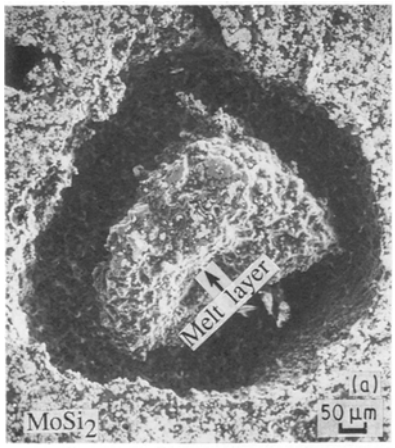

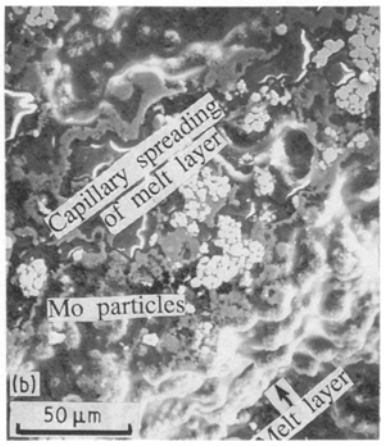

Figure 10(a) SEM of an unreacted portion surrounded by $MoSi_2$ product. Arrow indicates appearance of a melt layer. (b) Melt layer at the arrow in (a) at a higher magnification. Liquid Si spread into the voids of the compact and channels of solidified Si are visible after capillary spreading. Unreacted Mo particles with their original shape are also seen. (c) SEM of Mo particles in (b) at a higher magnification.

than the Mo particles (density of $MoSi_2$ is 6.29 g cm^{-3}, about 38% lower than the density of Mo). With an increase of the percentage TMD of the compact to 46% or above, unreacted portions and segregated areas disappeared completely, while a considerable reduction in porosity was observed (Fig. 11).

Surface structures of combustion-synthesized $MoSi_2$ compacts, as evidenced by scanning electron micrographs, indicate macropores as large as 150 μm (Fig. 12a) and micropores as small as 0.1 μm or less (Fig. 12b). Dense surface structure with a network of small pores and locally sintered areas are some of the unique surface structural features of combustion-synthesized compacts. This can be seen clearly in Fig. 12b at a magnification of × 500 and Fig. 12c at a magnification of × 5000. Assemblages of Mo particles coated with $MoSi_2$ product layer are noticeable in Fig. 12c, and none of the compacts examined under SEM indicated flaky or platelet morphology of Si particles even at a magnification of × 15 000.

Combustion-synthesized samples exhibited a layered structure as indicated in Fig. 13 along with a linear and a radial expansion. The linear expansion is about 10 to 20% while the radial expansion is less than 5%. Outgassing of the absorbed gases and oxide impurities present on the surfaces of the reactants contribute to the lengthening of the compact. Another factor contributing to the lengthening is the molar volume of the product. The formation and growth of $MoSi_2$ layer on the surface of Mo particles changes the lattice structure of Mo from a cubic pattern to a tetragonal structure with an accompanying increase in volume. Also, the density of Mo is 10.2 g cm^{-3} and the density of $MoSi_2$ is 6.29 g cm^{-3}.

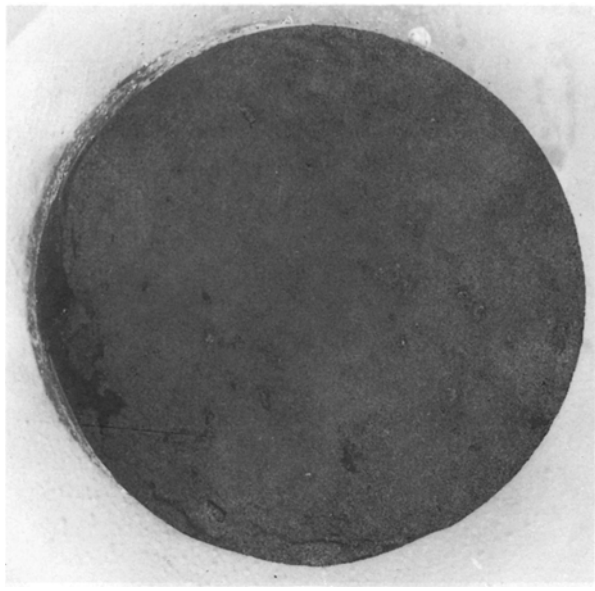

Figure 11 Optical micrograph of a combustion-synthesized $MoSi_2$ compact. Percentage TMD of compact prior to reaction = 46%.

4. Discussion

The reaction between Mo and Si in the combustion synthesis of $MoSi_2$ gives rise to a single end product, $MoSi_2$, without any intermediate products such as Mo_5Si_3 and Mo_3Si. In contrast, most silicide reactions involving Mo and Si powders [25, 26], and Si substrate and Mo film or Mo base material and $SiCl_4$ in H_2 atmosphere, give rise to products like $MoSi_2$, Mo_5Si_3 and Mo_3Si [27]. Products such as Mo_5Si_3 and Mo_3Si are not self-healing due to their low silicon contents and are deleterious since they cannot form a protective layer [28]. It is intriguing, therefore, to note that a single phase $MoSi_2$ can be obtained from the combustion synthesis reaction, which can possibly be

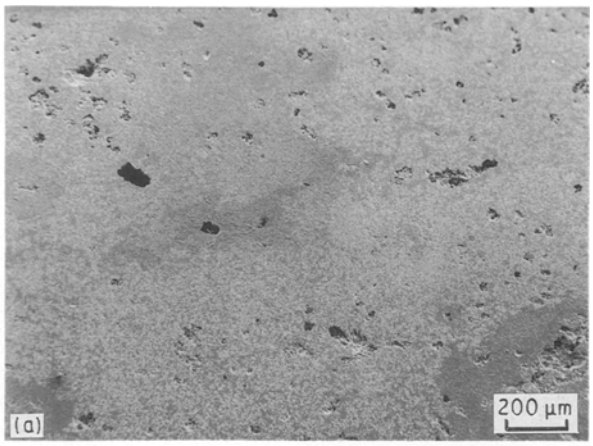

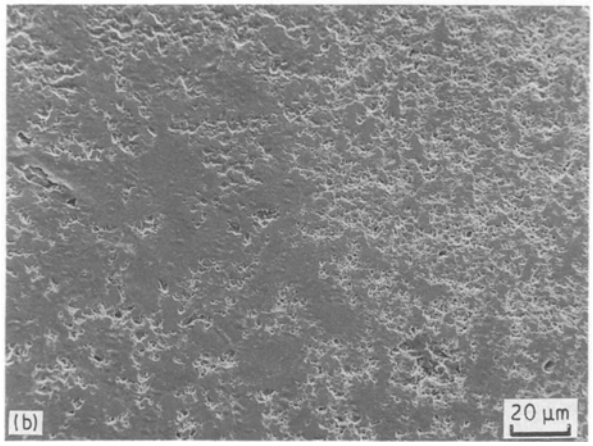

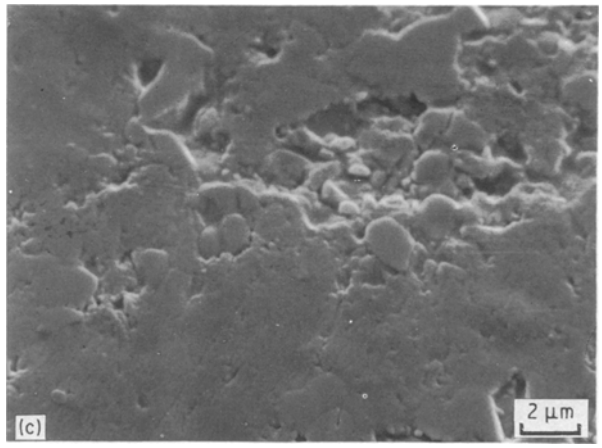

Figure 12 SEM of polished sample of combustion-synthesized $MoSi_2$. (a) Note the open pores with sizes as high as 150 μm at a magnification of × 50. (b) Fine porosity is visible at much higher magnification, × 500. (c) At still higher magnification, × 5000, assemblage of particles of $MoSi_2$ may be seen clearly.

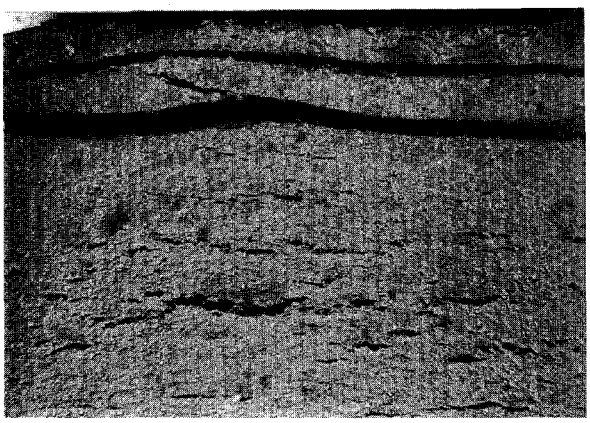

Figure 13 Layered appearance on the combustion-synthesized $MoSi_2$ compact.

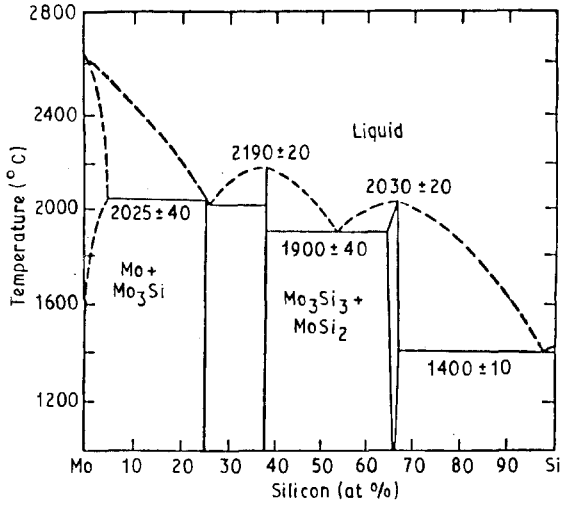

Figure 14 Equilibrium phase diagram of Mo–Si system [29].

used without loss of thermal, electrical, and self-healing properties for various applications. It should be noted that during the combustion reaction, only the sample temperature is above 1600 K and the surrounding chamber volume is at room temperature. In conventional industrial processes and in solid–solid diffusional reactions, for example the thermal explosion mode of combustion synthesis, the sample temperature would roughly be equal to the ambient temperature. The temperature difference between the sample and ambient is at least two orders of magnitude higher in the combustion-synthesis technique as opposed to conventional techniques. This is one of the attributes of the combustion-synthesis technique.

The mechanism of single-phase formation in combustion synthesis differs from that of solid–solid reactions occurring between Mo and Si particles or Si substrate and Mo film or layers. In the combustion-synthesis technique, the heating rates are high and diffusional and residence times are low, whereas in solid–solid reactions heating rates are low, and reaction times run for several hours. At a heating rate of 48 000 K min^{-1}, the diffusional reactions take place at an extremely fast rate in the combustion-synthesis technique. The phase diagram of Mo–Si (Fig. 14) indicates three different equilibrium products [29] and depending upon the particle size and rate of heating, three different products are possible. As we have indicated earlier, the temperature of the reaction is sufficiently higher than the melting point of the diffusing species (Si) and therefore liquid Si diffuses into Mo giving rise to the $MoSi_2$ phase. The heating rates involved in the combustion reactions are very high and since $MoSi_2$ forms in a narrow compositional range as shown by the equilibrium phase diagram of the Mo–Si system, the likelihood of secondary products is negligible.

Since the thermocouples are inserted to the centreline of the compact, it is reasonable to assume that adiabatic conditions exist in the interior of the compact and the temperatures indicated by the thermocouples are reasonable. The specific heat of argon contributes to the heat conduction mechanism in porous compacts. The temperature value would be lower in vacuum as compared to argon if part of the reactants did not participate in the reaction, and if intermediate or secondary products such as Mo_5Si_3 or Mo_3Si were formed instead of $MoSi_2$. As may be noted from the X-ray analysis presented earlier, some of the reactants did not participate in the reaction when the combustion synthesis was carried out in vacuum. This in turn reduced the heat of the reaction, which is observed as a reduction in the combustion temperature. In vacuum, conduction is mainly by particle–particle contact and therefore the sample remained at its maximum temperature for 7 s (Fig. 6). It is reasonable to expect that the diffusional reactions between Mo and Si are occurring at 1690 K even after the reaction front has propagated, increasing the conversion of reactants to the product. This indicates that at the combustion temperatures generated in vacuum and argon atmospheres, melting and capillary flow of Si are facilitated and the formation of $MoSi_2$ product layer on Mo particles is due to the diffusion of Si atoms into the lattice of Mo. The whole process is complete within a very short time (less than 1 min) after the reaction is initiated on the surface of the compact, in contrast to commercial manufacturing techniques which require operation of large industrial furnaces at high temperatures for several hours.

Our experiments with various combinations of Mo and Si particle sizes indicate that an optimum particle size of Si is present beyond which the combustion front cannot propagate. A summary of the observations with various particle sizes is given in Table IV. Decreasing the particle size of Mo to the range 4 to 8 μm from < 63 μm particles, while keeping the Si size constant at < 44 μm also exhibited 100% conversion efficiency (in argon atmosphere). But increasing the particle size of Si to < 150 μm (average particle size 43.5 μm) did not propagate the combustion wave fully. The reaction front was quenched after propagating to 4 mm. X-ray analysis of the interface showed reflections corresponding only to $MoSi_2$, Mo and Si. This observation is significant, implying that solid–solid diffusional reactions due to the diffusional fluxes ahead of the combustion zone were absent and that $MoSi_2$ forms in a single step from the reactants. If

solid–solid diffusional reactions were to play a significant role ahead of the reaction front, formation of lower silicides such as Mo_5Si_3 and Mo_3Si (Fig. 14) would have been observed when analysed by SEM in back-scattered mode and by X-ray diffractometry.

As can be noted from Table IV, the reaction proceeds to completion with larger particle size of Mo and smaller particle size of Si. But when the experiments were carried out with Mo powder and with < 300 μm Si powder, the reaction propagated only a few mm into the compact and a natural extinction of the front was observed. This is attributed to the lower rate of heat release with larger particle size of Si (and fine Mo powder) coupled with the heat losses due to the conduction of heat to the reactants ahead of the front. The limiting factor seems to be the time required for melting of Si and its subsequent diffusional reaction with Mo. Keeping the ignition coil on even after the reaction has initiated did not help substantially in sustaining the front and the effect was marginal (propagated to only 4 mm in length). Natural extinction or quenching phenomena provided an opportunity to determine the importance of diffusional reactions ahead of the reaction front, and to investigate whether an intermediate product exists at the interface between the $MoSi_2$ and the reactants.

X-ray characterization of the material scraped from the interface at which the reaction front extinguished revealed diffraction patterns representing $MoSi_2$, Mo and Si. This indicates that a single-step reaction leading to $MoSi_2$ is occurring during the synthesis. To prove this, quenching experiments were carried out by dropping the compact in liquid argon while the combustion front was propagating (the temperature of the liquid argon was ~ 90 K). Structural analysis of the material at the interface also indicated a single-phase $MoSi_2$, Mo, and Si, confirming that in combustion synthesis, $MoSi_2$ is formed in a single step. It also implies that diffusional fluxes ahead of the front are not high, and the time involved for the diffusional reactions ahead of the front is not sufficient enough to form a product such as Mo_5Si_3.

TABLE IV Effect of particle size of Si on the self-propagating behaviour of Mo–2Si mixture

Average particle size (μm)		Experimental observations on propagation of combustion wave
Mo	Si	
5.7	12.6	Self-sustaining combustion wave.
	43.5	Combustion wave propagated to 2–4 mm and extinguished.
	79.1[a]	Ignited with difficulty, combustion wave extinguished immediately after ignition.
13.3	12.6	Self-sustaining combustion wave.
	43.5[a]	Combustion wave propagated to 2–4 mm and extinguished.
	79.1[a]	Ignited with difficulty, combustion wave extinguished immediately after ignition.
18.6	12.6	Self-sustaining combustion wave.
	43.5[a]	Extinguished just after initiation of wave.
	79.1[a]	Extinguished just after initiation of wave.

[a] Prolonged radiative heating of the surface of the compact with an ignition coil did not increase the length of the propagation.

5. Conclusions

Single-phase $MoSi_2$ can be synthesized from elemental powders Mo and Si using the SHS technique. The combustion velocity increased with increase of percentage TMD, the diameter of the compact and the surrounding chamber pressure. The measured combustion temperature, 1886 K in argon, was close to the calculated adiabatic combustion temperature (1900 K) while the measured value in vacuum was lower by about 200 K. Microstructural examination of the compacts revealed unreacted and segregated areas, and with increased density a reduction in unreacted and segregated areas was observed. When compacts with a high percentage TMD (above 45%) were reacted in argon, locally sintered areas with a very low volume percentage of pores were observed.

X-ray diffraction analysis revealed that conversion is 100% that in argon, while maximum conversion was only 90% in vacuum. Chemical analysis of the combustion-synthesized $MoSi_2$ indicated that the product is much purer than the reactants, and a significant reduction of oxygen impurity has been observed. The mechanism of silicide formation is attributed to the reactive diffusion of liquid Si atoms into Mo at the combustion temperature. Solid–solid diffusional reactions of the combustion front seem to be insignificant at the heating rates involved in combustion-synthesis experiments.

6. Acknowledgements

The author gratefully acknowledges Professor C. K. Law, Department of Mechanical Engineering, University of California, Davis (now Professor in the Department of Aerospace and Mechanical Engineering at Princeton University) for his insights and support without which this work would not have been possible.

References

1. J. E. SPICE and L. A. K. STAVELEY, *J. Soc. Chem. Ind.* **68** (1949) 313.
2. *Idem, ibid.* **68** (1949) 348.
3. F. BOOTH, *Trans. Farad. Soc.* **49** (1953) 272.
4. A. G. MERZHANOV and I. P. BOROVINSKAYA, *Dokl. Akad. Nauk. S.S.S.R.* **204** (1972) 366.
5. *Idem, Comb. Sci. Tech.* **10** (1975) 195.
6. W. L. FRANKHOUSER, K. W. BRENDLEY, M. C. KIESZEK and S. T. SULLIVAN, "Gasless Combustion Synthesis of Refractory Compounds" (Noyes, New Jersey, 1985) pp. 3–79.
7. In Proceedings of DARPA/Army Symposium on Self-Propagating High Temperature Synthesis, Daytona Beach, Florida, October 1985 (US Government Printing Press, USA).
8. J. B. HOLT and Z. A. MUNIR, *J. Mater. Sci.* **21** (1986) 251.
9. P. D. ZAVITSOMOS and J. R. MORRIS, Jr., *Proc. Ceram. Engng Sci.* (1984) 625.

10. "Coatings of High Temperature Materials", edited by H. H. Hausner (Plenum, New York, 1966).
11. J. PARE and G. ELKUND, *Met. Prog.* (1978) 32.
12. J. SCHLICHTING, *High Temp.–High Press.* **10** (1978) 241.
13. "Kanthal Super Electric Heating Elements" (Kanthal Corporation, Bethel, Connecticut) (USA).
14. J. MILNE, "Instant Heat" (Kinetic Metals, Inc., Derby, Connecticut, 1985).
15. D. H. KILLEFFER and A. LINZ, "Molybdenum Compounds: Their Chemistry and Technology" (Interscience, New York, 1952).
16. R. WEHRMAN, in "High Temperature Materials and Technology", edited by I. E. Campbell and E. M. Sherwood (Wiley, New York, 1967) pp. 399–430.
17. B. ARONSSON, T. LUNDSTROM and S. RUNDQUIST, "Borides, Silicides and Phosphides" (Wiley, New York, 1965).
18. D. A. ROBINS and I. JENKINS, in "Plansee Proceedings", edited by P. Benesovsky (1955).
19. D. A. ROBINS and I. JENKINS, *Acta Metall.* **3** (1955) 598.
20. P. GRIEVSON and C. B. ALCOCK, in "Special Ceramics", edited by P. Popper (Academic, New York, 1960).
21. A. R. SARKISYAN, S. K. DOLUKHANYAN, I. P. BOROVINSKAYA and A. G. MERZHANOV, *Fizika Goreniya i Vzryva* **14** (1978) 49.
22. Powder Diffraction Files, File 6-0681 (International Joint Committee on Powder Diffraction Standards, Philadelphia, USA, 1988).
23. L. PAULING, in "Molybdenum Compounds: Their Chemistry and Technology", edited by D. H. Killeffer and A. Linz (Interscience, New York, 1952).
24. G. V. SAMSONOV and I. M. VINITSKII, "Handbook of Refractory Compounds", translated from the Russian by K. Shaw (IFI/Plenum, New York, 1980) p. 105.
25. G. V. SAMSONOV, "Silicides and their uses in Engineering" (Akad. Nauk. Ukr. SSR, Kiev, 1959) p. 44, pp. 106–112.
26. I. E. CAMPBELL and E. M. SHERWOOD, "High Temperature Materials and Technology" (Wiley, New York, 1967) p. 401.
27. S. P. MURARKA, "Silicides for VLSI Applications" (Academic, New York, 1983) pp. 29–131.
28. R. HENNE and W. WEBER, *High Temp.–High Press.* **18** (1986) 223.
29. L. BREWER, R. H. LAMOREAUX, R. FERRO, R. MARAZZA and K. GIRGIS, "Molybdenum: Physico–Chemical Properties of its Compounds and Alloys", edited by L. Brewer (International Atomic Energy Agency, Vienna, 1980).

Received 14 May
and accepted 26 June 1990